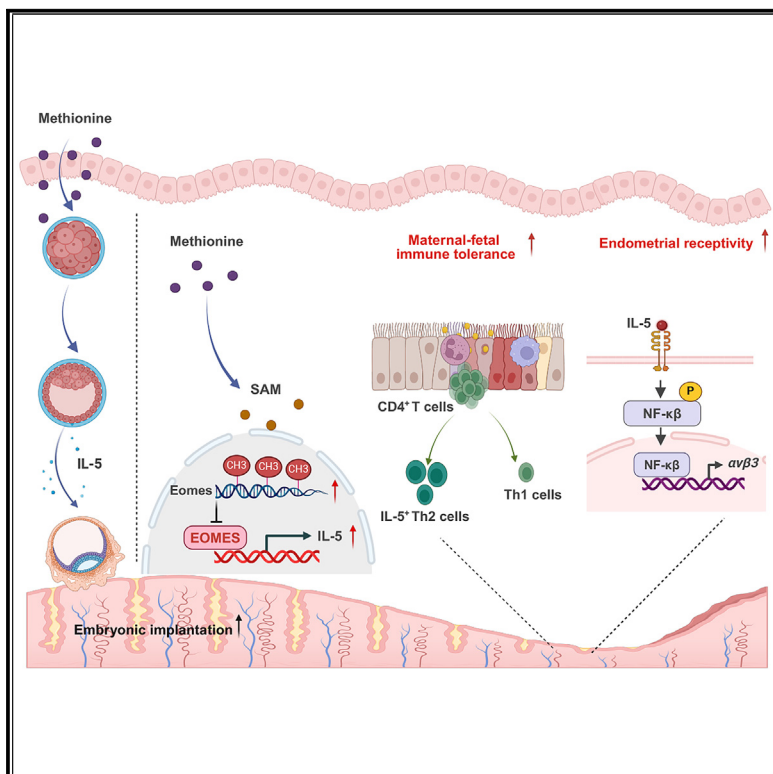


Methionine regulates maternal-fetal immune tolerance and endometrial receptivity by enhancing embryonic IL-5 secretion

Graphical abstract



Authors

Shuang Cai, Bangxin Xue, Siyu Li, ..., Haitao Yu, Shiyuan Qiao, Xiangfang Zeng

Correspondence

zengxf@cau.edu.cn

In brief

Cai et al. demonstrate that methionine-mediated IL-5 secretion activates the NF-κB pathway and enhances integrin $\alpha v\beta 3$ expression in endometrial cells, which improves endometrial receptivity. Meanwhile, methionine can also increase Th2 cells at the implantation sites by regulating IL-5 secretion, thus favoring maternal-fetal immune tolerance.

Highlights

- Methionine induces embryonic IL-5 secretion and improves embryonic development
- Methionine influences the DNA methylation of *Eomes*, which inhibits IL-5 transcription
- Methionine enhances the conversion of CD4⁺ T cells to IL-5⁺ Th2 cells through IL-5
- IL-5 improves endometrial receptivity by activating NF-κB pathway



Article

Methionine regulates maternal-fetal immune tolerance and endometrial receptivity by enhancing embryonic IL-5 secretion

Shuang Cai,^{1,2} Bangxin Xue,^{1,2} Siyu Li,^{1,2} Xinyu Wang,^{1,2} Xiangzhou Zeng,^{1,2} Zhekun Zhu,^{1,2} Xinyin Fan,^{1,2} Yijin Zou,^{1,2} Haitao Yu,^{1,2} Shiyuan Qiao,^{1,2} and Xiangfang Zeng^{1,2,3,*}

¹State Key Laboratory of Animal Nutrition and Feeding, Ministry of Agriculture and Rural Affairs Feed Industry Center, China Agricultural University, Beijing, China

²Frontier Technology Research Institute of China Agricultural University in Shenzhen, Shenzhen, China

³Lead contact

*Correspondence: zengxf@cau.edu.cn

<https://doi.org/10.1016/j.celrep.2025.115291>

SUMMARY

Endometrial receptivity and maternal-fetal immune tolerance are two crucial processes for a successful pregnancy. However, the molecular mechanisms of nutrition involved are largely unexplored. Here, we showed that maternal methionine supply significantly improved pregnancy outcomes, which was closely related to interleukin-5 (IL-5) concentration. Mechanistically, methionine induced embryonic IL-5 secretion, which enhanced the conversion of CD4⁺ T cells to IL-5⁺ Th2 cells in the uterus, thereby improving maternal-fetal immune tolerance. Meanwhile, methionine-mediated IL-5 secretion activated the nuclear factor κB (NF-κB) pathway and enhanced integrin αvβ3 expression in endometrial cells, which improved endometrial receptivity. Further, methionine strongly influenced the DNA methylation and transcription levels of the transcription factor eomesodermin (*Eomes*), which bound directly to the IL-5 promoter region and inhibited IL-5 transcription. Methionine modulated IL-5 transcription, maternal-fetal immune tolerance, and endometrial receptivity via its effects on *Eomes*. This study reveals the crucial functions of methionine and IL-5 and offers a potential nutritional strategy for successful pregnancy.

INTRODUCTION

Maternal-fetal immune tolerance and endometrial receptivity are essential for a successful pregnancy. Recognition of the allogeneic fetus and tolerance of the maternal immune system of the allogeneic fetus and maternal-fetal immune tolerance are notable exceptions of the immunological principles.^{1,2} Impaired maternal-fetal immune tolerance may lead to adverse pregnancy outcomes, such as recurrent spontaneous abortion, assisted reproduction failure, intrauterine growth restriction, and placental insufficiency. In fact, about 60% of recurrent spontaneous abortions are caused by immune abnormalities, including antiphospholipid syndrome, abnormal immune cells, and cytokine imbalance.³ Trophoblast cells play a critical role in maintaining maternal-fetal immune tolerance and carry out this function by expressing and secreting various chemokines and cytokines.⁴ In particular, during the embryonic implantation phase, Th1/Th2 cytokine balance affects maternal-fetal immune tolerance and endometrial receptivity, which are important for successful implantation. Elevated levels of Th1 cytokines are associated with rejection of embryos, while elevated Th2 cytokine levels are associated with pregnancy.^{5,6}

In addition to cytokines and cytokine receptors, various other factors are involved in the maintenance and success of preg-

nancy, such as hormones, genetic factors, and one-carbon nutrients. With regard to one-carbon nutrients, it has been reported that the supply of maternal methyl group donors (methionine, betaine, choline, and folate) before and during pregnancy may regulate embryonic cell fate⁷ and that disorders in one-carbon metabolism can lead to impaired blastocyst development and reproductive performance in mice and sows.⁸ For example, folate has been found to ameliorate neural tube defects,⁹ fetal malformations,¹⁰ premature spontaneous abortion,¹¹ pregnancy hypertension syndrome, and megaloblastic anemia.¹² Further, *in utero* exposure to choline is known to improve visual memory through cholinergic transmission and epigenetic mechanisms, defined as stable, heritable phenotypic changes caused by chromosomal alterations rather than changes in DNA sequence, and it can also decrease the risk of congenital heart defects.^{13,14} Methionine, an essential amino acid, and its metabolism and biological function have been explored in the context of aging, metabolic disorders, cancer, and reproduction, and maternal supplementation with methionine has been found to ameliorate some fetal deformities.¹⁵ In addition, our previous studies have confirmed the role of methionine in early embryonic development,^{16,17} but its potential role in maternal-fetal immune tolerance and endometrial receptivity is unclear.



Methionine plays an important role in methylation, redox maintenance, polyamine synthesis, and immune regulation.¹⁸ Previous studies have shown that tumor cells exhibit high methionine cycle flux and a remarkable dependency on methionine, as tumor load is dramatically decreased by 94% under methionine starvation conditions.¹⁹ In contrast, other amino acids, such as threonine, leucine, and tryptophan, have no such effect. In addition, a methionine-restricted diet has been shown to suppress tumor growth and sensitize tumors to apoptosis-inducing chemotherapy and radiation therapy in various cancer types and mouse models.^{20–22} On one hand, the methionine cycle flux specifically influences the transmethylation rates and epigenetic state of cancer cells and drives tumor initiation.²³ On the other hand, tumor cells avidly consume and outcompete T cells for methionine via high expression of the methionine transporter SLC43A2, and this results in loss of histone H3 lysine 79 dimethylation (H3K79me2) and impaired T cell immunity.^{24,25} Genetic ablation of SLC43A2 in cancer cells has been found to restore methionine metabolism in T cells, thus increasing the intercellular levels of S-adenosylmethionine (SAM), a derivative of methionine, and yielding H3K79me2.²⁶ The findings of these studies indicate that methionine affects growth and immune escape in tumor cells by regulating histone modifications. Early embryonic development and tumor formation share similar immunological escape mechanisms, which regulate the host's immune tolerance of embryonic and tumor cells.^{27,28} Accordingly, our previous studies have confirmed that methionine supplementation during early pregnancy enhances the expression of methionine adenosyltransferase 2A and improves DNA synthesis by activating the SAM sensor upstream of mTORC1/mTORC1/S6K1/carbamoyl-phosphate synthetase 2 pathway during early embryonic development.^{16,17} However, whether methionine influences early embryonic methylation and cytokine secretion remains unclear. In this study, we tried to answer this question by identifying the roles of methionine in cytokine secretion and the related mechanisms. Our findings in rat and pig models demonstrated that methionine played a predominant role in embryonic development and implantation and pregnancy outcomes. Further, our mechanistic experiments showed that these effects of methionine were mediated by the DNA methylation of *Eomes*, which subsequently affected the expression of interleukin-5 (IL-5) in early embryonic trophoblast cells. IL-5 activated the nuclear factor κB (NF-κB) pathway to promote integrin αvβ3 expression and enhanced the conversion of CD4⁺ T cells to IL-5⁺ Th2 cells in the uterus, thereby improving maternal-fetal immune tolerance and endometrial receptivity to benefit embryonic implantation. This novel function of methionine and IL-5 shows great potential to improve reproductive health for mammalian animals and human beings.

RESULTS

Methionine improves embryonic development and pregnancy outcomes

To reveal the critical role of one-carbon nutrients in early embryonic development, 220 pregnant rats were fed *ad libitum* one of 22 diets consisting of varying levels of folate, betaine, choline, and methionine (Figure 1A). These dietary compositions were

created using central composite design (CCD). CCD is a state-space modeling approach that explores how an animal responds to the problem of balancing multiple and changing nutrient needs in a multidimensional and variable nutritional environment. The CCD considers nutrients as an n-dimensional space in which the n components are represented by separate axes.²⁹ The number of implantation sites, uniformity of embryonic implantation, concentration of SAM, S-adenosylhomocysteine (SAH), and SAM/SAH ratio in serum were plotted as response surfaces mapped onto diet composition space and interpreted statistically using Design-Expert (v.10.0.7). To aid interpretation, the data surfaces were presented as 2D nutrient heatmaps cut through the response surface at the medium of the other two nutrient axes.³⁰ Our results showed that the number of implantation sites was influenced by all four nutrients, but methionine gave the strongest effect (Figure 1B). The effect of choline, betaine, and folate on embryonic implantation and the uniformity of embryo implantation was relatively marginal when the methionine level was adequate (Figure 1C). SAM and SAH are important in regulating the methylation of DNA and histones.^{31,32} To investigate the role of one-carbon nutrients in transmethylation efficiency during early pregnancy, we analyzed the concentrations of SAM and SAH and calculated the SAM/SAH ratio in serum. The results showed that methionine had a stronger effect on the SAM/SAH ratio than betaine, folate, and choline (Figures 1D, S1A, and S1B). These results collectively indicate that methionine plays a predominant role among one-carbon nutrients during early pregnancy.

To directly verify the influence of methionine on embryonic development and implantation, we collected rat zygotes for culture *in vitro* and added 50, 62.5, 75, 87.5, and 100 μM methionine to the medium. The results showed that 75 and 87.5 μM methionine supplementation in the medium significantly increased the blastocyst rate in rat embryo culture (Figure 1E). Furthermore, we fed rats a 0% or 1.0% methionine diet during early pregnancy and found that methionine supplementation resulted in an increase in the number of implantation sites (Figure 1F). Similarly, in the case of pigs, 0.2% methionine supplementation during early pregnancy influenced the concentrations of SAM and SAH in serum (Figures S1C and S1D) and increased the litter size and live litter size (Figures S1E and S1F). To further explore the influence of methionine on pregnancy outcomes, we supplemented rats with a diet deprived of methionine during early pregnancy (referred to as short term) or throughout the entire pregnancy (referred to as long term) (Figure 1G). The parturition rate, referring to the rate of pup delivery, was 65.12% and 35.56% in the short-term and long-term groups, respectively, while that of the methionine-supplemented control group was 80.65%. Compared with the control group, the litter size and live litter size were significantly reduced in both methionine deprivation groups (Figures 1H and 1I), and the average birth weight of newborns drastically decreased when methionine was deprived long term (Figure 1J). In addition, an increasing tendency for large variations in birth weight of methionine-deprived rats was observed (Figure S1G).

To further study the influence of methionine on reproductive health of progenies, all female offspring of the three groups of rats with or without experiencing short- or long-term methionine

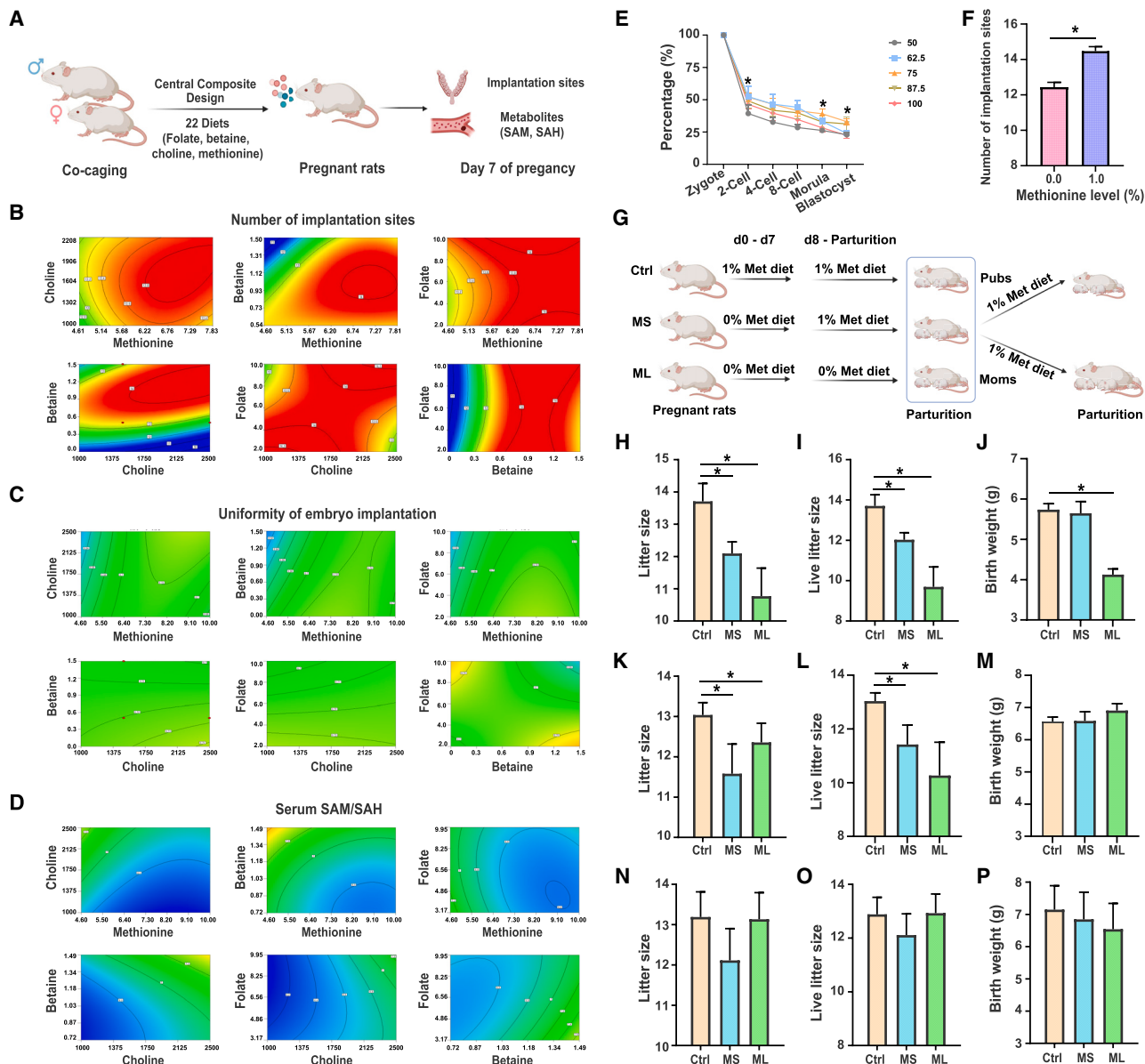


Figure 1. Methionine improved embryonic development and pregnancy outcomes

- (A) A schematic depiction of the experimental settings. Pregnant rats were fed with one of the 22 diets consisting of varying levels of folate, betaine, choline, and methionine from day 1 to day 7 of pregnancy.
- (B) Response surfaces showing the relationship between the number of implantation sites versus one-carbon nutrient content of the diet. Surfaces were fitted using generalized additive models with thin-plate splines. Six 2D slices are given to show all four nutrient dimensions. For each 2D slice, the other two factor is at its median. In all surfaces, red indicates the highest value, while blue indicates the lowest value, with the colors standardized across the six slices.
- (C) Response surfaces showing the relationship between the uniformity of embryonic implantation versus one-carbon nutrient content of the diet.
- (D) Response surfaces showing the relationship between the serum SAM/SAH ratio versus one-carbon nutrient content of the diet.
- (E) Blastocyst rate of zygotes treated with different methionine concentrations.
- (F) The number of implantation sites for rats fed a methionine supplementation diet during early pregnancy.
- (G) A schematic of the experimental settings. Pregnant rats were fed a diet deprived of methionine during early pregnancy or throughout the entire pregnancy. All female offspring were followed up, fed an identical standard diet containing sufficient methionine, and observed for their pregnancy performance.
- (H–J) The reproductive performance of rats that were deprived of methionine during early pregnancy or throughout pregnancy.
- (K–M) The reproductive performance of rats' offspring.
- (N–P) The reproductive performance of rats for the second round of pregnancy.
- n* = 15. **p* < 0.05. Data are mean ± SEM. See also Figure S1.

deprivation were followed up, fed an identical standard diet containing sufficient methionine, and observed for their pregnancy performance. Compared with the control group, both the litter size and live litter size were decreased in offspring whose mothers underwent short-term or long-term methionine deprivation (Figures 1K and 1L). The average birth weight and variable coefficient of birth weight of newborns showed no difference (Figures 1M and S1H).

After weaning, the original dams underwent a second round of pregnancy and were fed the same diet containing a sufficient amount of methionine. However, there was no significant difference in litter size, live litter size, birth weight, or variable coefficient of birth weight among the three groups (Figures 1N–1P and S1I). These results collectively indicated that methionine status is critical for pregnancy health of not only mothers but also their offspring.

Methionine enhances embryonic IL-5 secretion and immune homeostasis at the maternal-fetal interface

To clarify the effects of methionine on immune status during pregnancy, we measured the serum concentrations of cytokines in pigs fed diets with different methionine levels. The correlation analysis of serum cytokine levels with litter size, live litter size, healthy piglets, and birthweight showed that the serum IL-5 level was closely related to the reproductive performance of sows (Figure 2A). In addition, single-cell sequencing for porcine embryos showed that IL-5 expression was higher in good-quality embryos compared with poor-quality embryos (Figure 2B). IL-5 was primarily expressed in extra-embryonic cells, including extravillous trophoblast, syncytiotrophoblast, trophectoderm, and cytotrophoblast (Figure 2B). These results indicated that IL-5 was a critical factor affecting embryonic development and implantation.

Compared with the control group, the concentration of methionine, SAM, and IL-5 in serum and uterine fluid of rats fed methionine was significantly increased during embryonic implantation (Figures 2C–2H and S2A–S2F). The results of immunofluorescence staining of IL-5 in rat blastocysts showed that methionine supplementation significantly increased the expression of IL-5 in blastocysts (Figures 2I and 2J). In addition, compared with the methionine deprivation group, the secretion of IL-5 in trophoblast cells of humans and rats treated with appropriate methionine was increased, while supplementation with the methionine inhibitor ethionine reduced IL-5 secretion (Figures S2G and S2H).

IL-5, a cytokine produced by Th2 cells, is integral to maternal-fetal immune tolerance. To evaluate the role of methionine in immune homeostasis, the molecular markers of Th1 and Th2 immune cells were detected at the maternal-fetal interface of pregnant rats fed different levels of methionine. The results showed that methionine supplementation significantly increased the number of Th2 cells (Figure 2K). Furthermore, CD4⁺ T cells were isolated from mouse uterine tissues and divided into six treatments: (1) methionine-deficient, (2) methionine-supplemented, (3) recombinant murine IL-5, (4) trophoblast cells culture supernatant, (5) supernatant from trophoblast cells treated with methionine, and (6) supernatant from trophoblast cells treated with methionine and neutralizing anti-IL-5 monoclonal antibody (mAb). The results showed that methionine significantly

enhanced the conversion of CD4⁺ T cells to IL-5⁺ Th2 cells by promoting the secretion of IL-5 from trophoblast cells (Figures 2L–2N). Collectively, these results suggested that methionine enhanced the secretion of IL-5 in trophoblast cells, improving immune homeostasis at the maternal-fetal interface.

Methionine regulates the uterine NF-κB pathway and maternal-fetal immune tolerance through IL-5

To further verify the influence of IL-5 on embryonic implantation, we established *in vitro* implantation models of human and porcine embryos with IL-5 knockout. The results showed that methionine supplementation significantly increased the embryo adhesion rate, while IL-5 knockout impaired embryonic implantation for both human and porcine embryos (Figures 3A and S3A). To uncover the mechanisms by which methionine-regulated IL-5 secretion promoted embryonic implantation, we detected the activation of NF-κB pathways regulated by cytokines as well as the expression of the essential endometrial receptivity genes LIF, HOXA1, and integrin $\alpha v\beta 3$ in implantation site tissues of rats fed different levels of methionine during pregnancy. The result showed that 1.0% methionine dietary supplementation significantly increased the expression of IL-5, IL-5RA, p65 NF-κB, and integrin $\alpha v\beta 3$ (Figures S3B and S3C). In addition, we treated human and porcine endometrial cells with the supernatants from IL-5 knockout and methionine pre-treated trophoblast cells. We found that methionine supplementation significantly increased the expression of p65 NF-κB and integrin $\alpha v\beta 3$ in endometrial cells (Figures 3B, 3C, S3D, and S3E), indicating activation of the NF-κB pathway and improvement of endometrial receptivity. However, in IL-5 knockout-treated groups, the expression of p65 NF-κB and integrin $\alpha v\beta 3$ was sharply decreased compared with the control group, which was consistent with the adhesion rate (Figures 3B, 3C, S3D, and S3E). These results suggested that methionine might activate the NF-κB pathway through IL-5, thereby enhancing the expression of integrin $\alpha v\beta 3$ and improving embryonic implantation.

To confirm the critical role of methionine-mediated activation of NF-κB in embryonic implantation, we treated human and porcine trophoblast cells with methionine and, at the same time treated endometrial cells with IL-5RA knockout and an NF-κB inhibitor and then carried out an *in vitro* implantation simulation test. As shown in Figures 3D and S3F, methionine supplementation significantly increased the adhesion rate, while IL-5RA knockout and NF-κB inhibitor treatment impaired embryonic implantation compared with the control group. In addition, similar changes of the expression of p65 NF-κB and integrin $\alpha v\beta 3$ were noticed in human and porcine endometrial cells in *in vitro* embryo implantation models (Figures 3E, 3F, S3G, and S3H) and *in vitro* culture of rat uterine tissue (Figures S3I and S3J). These results indicated that methionine-mediated IL-5 secretion was sensed by IL-5RA in the uterus to activate the NF-κB pathway, which enhanced integrin $\alpha v\beta 3$ expression to improve endometrial receptivity.

To explore the effects of embryonic and maternal IL-5 on embryonic implantation, zygotes were collected, microinjected with IL-5 or a neutralizing anti-IL-5 mAb, and then transferred into pseudopregnant $Il-5^{-/-}$ or wild-type mice (Figure 3G). Compared with the control group, the number of implantation

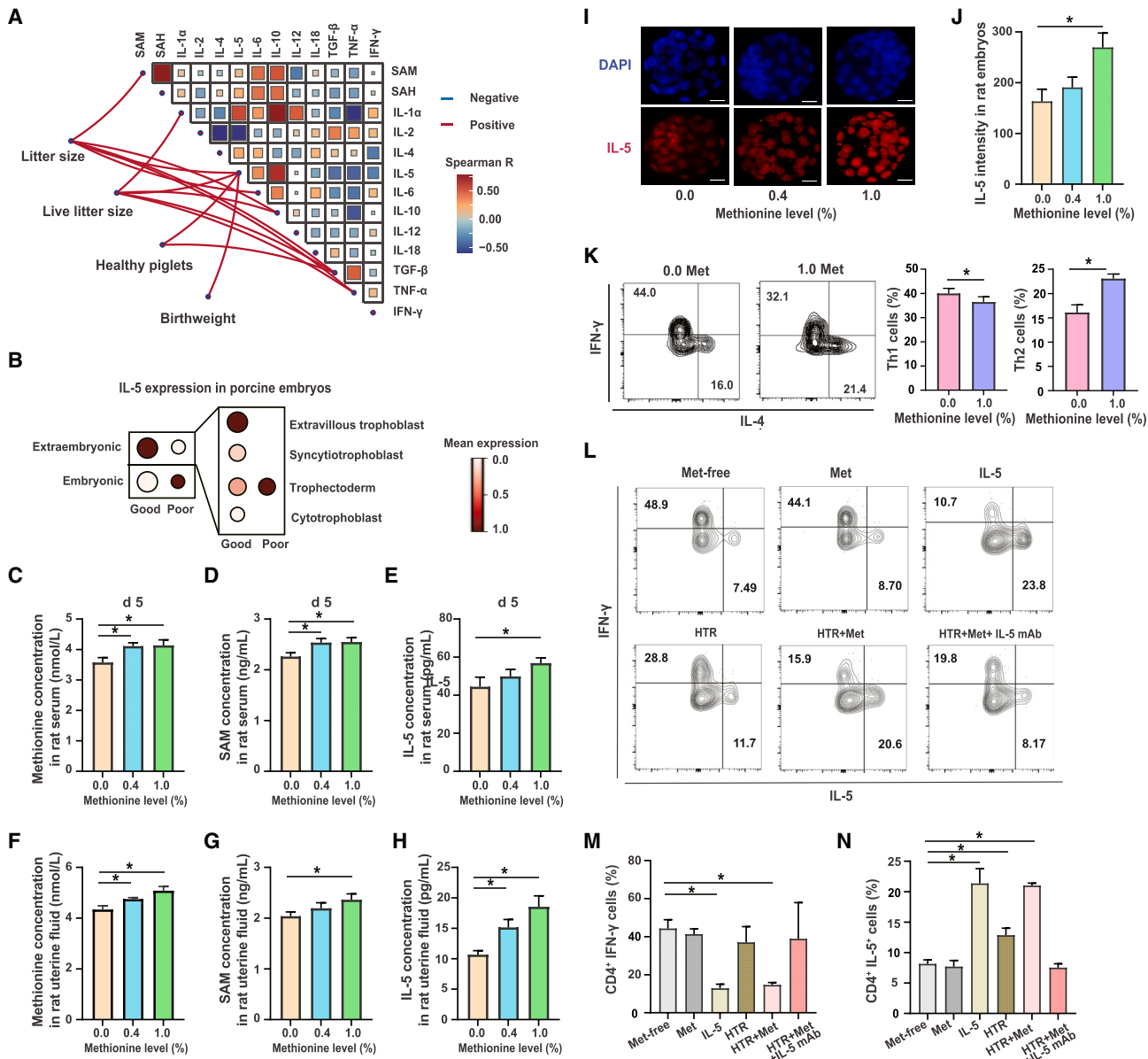


Figure 2. Methionine enhanced embryonic IL-5 secretion and immune homeostasis at the maternal-fetal interface

(A) Correlation plot of the serum cytokines, methionine metabolites, and reproductive performance for sows. The sizes of dots indicate the degree of the correlation. Statistically significant correlations are displayed. The red dots indicate a positive correlation, while the blue dots indicate a negative correlation.

(B) IL-5 expression in porcine embryos.

(C–E) Serum methionine, SAM, and IL-5 concentrations in rats fed methionine on day 5 of pregnancy.

(F–H) Methionine, SAM, and IL-5 concentrations in uterine fluid of rats fed methionine on day 5 of pregnancy.

(I and J) Immunofluorescence staining and intensity of IL-5 (red) and DAPI (blue) in blastocysts of rats fed different methionine diets. $n = 12$. Scale bar: 50 μ m

(K) The number of Th1 and Th2 cells in the maternal-fetal interface of pregnant rats fed different levels of methionine.

(L–N) The number of CD4 $^+$ Th1 cells and CD4 $^+$ IL-5 $^+$ cells in CD4 $^+$ T cells isolated from mouse uterine tissue and treated with methionine, recombinant murine IL-5, and the culture medium supernatant of trophoblast cell pre-treated with methionine or a combination of methionine and neutralizing anti-IL-5 mAbs.

Data are mean \pm SEM of at least three independent experiments. * $p < 0.05$. See also Figure S2.

sites in $Il-5^{-/-}$ or wild-type mice was sharply decreased in the IL-5 mAb injection group, while the number of implantation sites in the IL-5 injection group was significantly increased (Figure 3H). In addition, we focused on the maternal-fetal interface and injected IL-5 or a neutralizing anti-IL-5 mAb into the uterine horns.

Compared with the control group, IL-5 injection significantly increased the number of implantation sites and the expression of p65 NF- κ B and integrin $\alpha v \beta 3$ (Figures 3I–3K), indicating that IL-5 derived from the embryo or mother had the same function, both improving embryonic implantation.

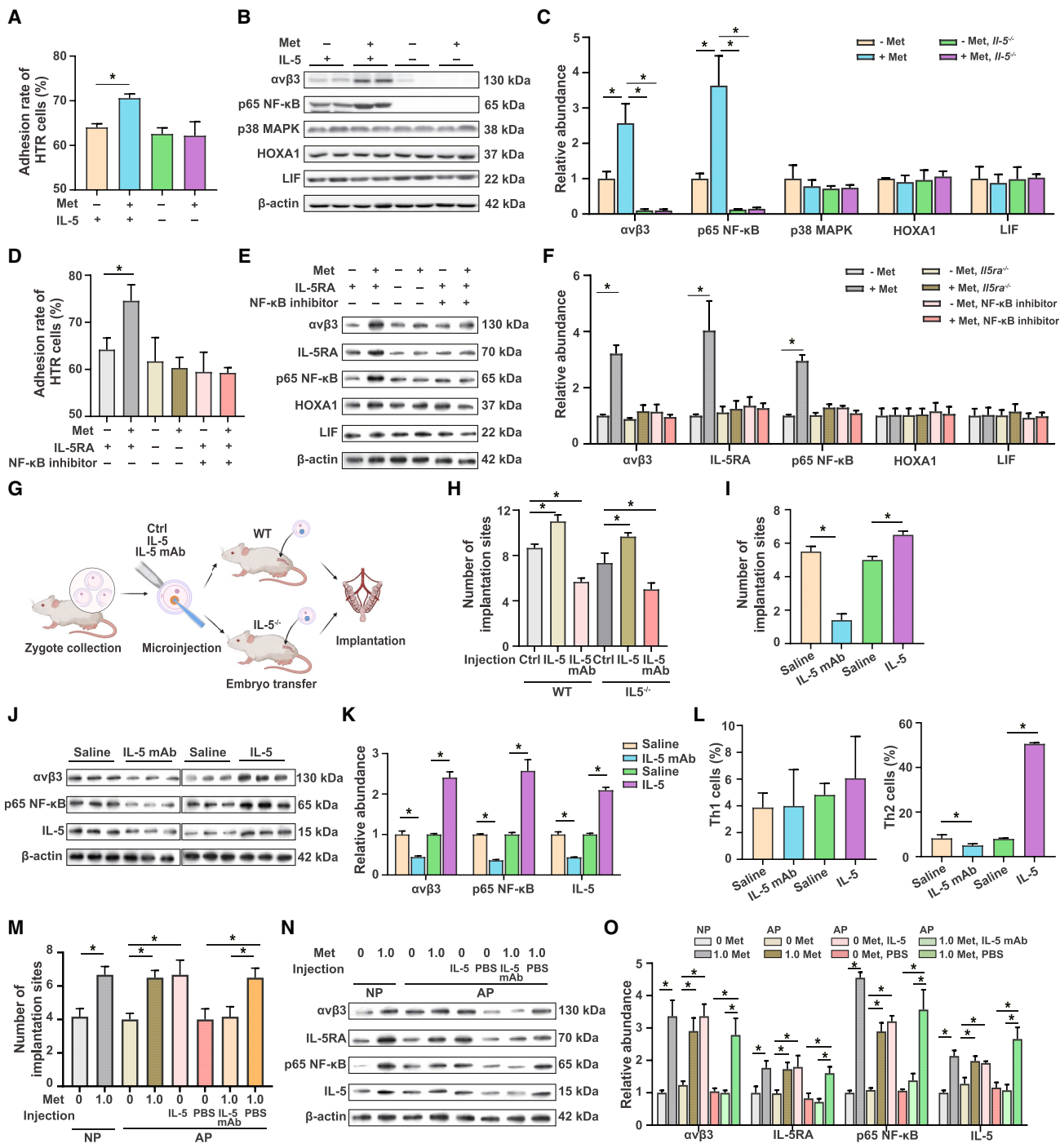


Figure 3. Methionine regulated the uterine NF-κB pathway and maternal-fetal immune tolerance through IL-5

(A) The adhesion rate for human trophoblast cells treated with methionine and IL-5 knockout.

(B and C) IL-5 knockout human trophoblast cells were treated with methionine for 24 h, and then the supernatants were collected and used to treat endometrial cells for another 24 h. Shown is western blot analysis for LIF, HOXA1, integrin $\alpha v\beta 3$, p65 NF- κ B, and p38 mitogen-activated protein kinase (MAPK) in human endometrial cells.

(D) The adhesion rate for human trophoblast cells treated with methionine and endometrial cells treated with IL-5RA knockout or NF- κ B inhibitor.

(E and F) Western blot analysis for IL-5RA, LIF, HOXA1, integrin $\alpha v\beta 3$, and p65 NF- κ B in *in vitro* implantation simulation tests with human trophoblast cells treated with methionine and endometrial cells treated with IL-5RA knockout and NF- κ B inhibitor.

(G) A schematic of the experimental settings. Zygotes were collected and microinjected with control H₂O, IL-5, and a neutralizing anti-IL-5 mAb and then transferred into pseudopregnant $II-5^{-/-}$ or WT mice.

(legend continued on next page)

To evaluate the role of IL-5 in maintaining maternal-fetal immune tolerance, we detected the molecular markers at the maternal-fetal interface in rats injected with IL-5 and a neutralizing anti-IL-5 mAb at the uterine horns. The result demonstrated that IL-5 injection significantly increased the number of Th2 cells at the maternal-fetal interface compared to the control group, while neutralizing anti-IL-5 mAb injection significantly reduced the Th2 cell numbers (Figure 3L), indicating that IL-5 played a critical role in maternal-fetal immune tolerance. In addition, we established a well-recognized murine model of immunological spontaneous abortion. In this model, an abnormal maternal immune response led to the rejection of fetuses and spontaneous abortion in the CBA Jackson laboratory mouse (CBA/J) × dissociation of base analog 2 Jackson laboratory mouse (DBA/2J) group (allogeneic pregnant [AP]), but not in the CBA/J × BALB/c group (syngeneic pregnant). We fed pregnant AP mice with diets containing different levels of methionine and administered intraperitoneal injections of IL-5, neutralizing anti-IL-5 mAbs, and PBS to explore the effects of methionine and IL-5 on maternal-fetal immune tolerance. The results showed that methionine supplementation and IL-5 injection significantly increased the number of implanted embryos and enhanced NF- κ B phosphorylation and $\alpha\beta\beta$ expression (Figures 3M–3O). Taken together, these results indicated that methionine-mediated IL-5 secretion activated the NF- κ B pathway and improved maternal-fetal immune tolerance.

Methionine enhances IL-5 transcription by regulating methylation of the transcription factor Eomes

IL-5 was primarily expressed in trophoblast cells. To examine the utilization of methionine in trophoblast cells, we cultured porcine trophoblast cells in the presence of L-methionine-1-13C-[methyl-D³] labeled with carbon-13 and tritium (hydrogen-3) and determined the distribution of methionine in cellular nucleic acid and proteins as described previously (Figure 4A).³³ Our data showed that carbon-13 of methionine contributed 41.83% of nucleic acid (DNA, 21.32%; RNA, 20.51%) and 14.94% of proteins, while the methyl-D³ group of methionine accounted for 41.79% of nucleic acid (DNA, 21.82%; RNA, 19.97%) and 18.88% of cell proteins (Figure 4B). Consistently, in rat blastocysts, histone H3 lysine 4 trimethylation (H3K4me3) was significantly increased in the 1.0% methionine group, while no significant difference was observed with histone H3 lysine 9 trimethylation or histone H3 lysine 27 trimethylation compared to the methionine deficiency group. Additionally, the intensity of 5-methylcytosine decreased while 5-hydroxymethylcytosine increased in response to 1.0%

methionine in comparison with the methionine deprivation group (Figure S4A).

To systematically understand the function and regulatory roles of methionine on DNA and H3K4 methylation in the blastocyst, we profiled the DNA and H3K4 methylomes and transcriptome of blastocysts collected from rats fed different methionine diets during pregnancy. Genome-wide DNA methylation was revealed through whole-genome methylation sequencing (WGBS). A total of 1.32 billion paired-end reads covering 187 Gb of sequence from WGBS were generated, resulting in an average mapping rate of 62% to the reference genome (Table S1). Our results indicated that the CpG island, exons, introns, promoters, 3' untranslated region (UTR), and 5' UTR were mostly hypermethylated in methionine-deprived blastocysts but mostly hypomethylated in blastocysts of rats supplemented with 1.0% methionine (Figure S4B). The histone methylation pattern of H3K4me3 was revealed through ultra-low-input native chromatin immunoprecipitation sequencing (ChIP-seq). We found that H3K4me3 was mostly enriched in the promoters, introns, and distal intergenic regions in blastocysts of methionine-supplemented rats (Figure S4C). Furthermore, we performed RNA sequencing (RNA-seq) to investigate the effects of methionine on the transcriptome profile of rat blastocysts supplemented with or without methionine. A total of 371 differentially expressed transcripts were identified. Of the H3K4 methyltransferases, *Kmt2a*, *Kmt2b*, *Kmt2c*, *Kmt2d*, and *Kmt2e* were significantly upregulated, while H3K4 demethylation-associated enzymes, such as *Kdm1a*, *Kdm5a*, *Kdm5b*, *Kdm5c*, and *Kdm5d*, were downregulated in 1.0% methionine-supplemented blastocysts (Figure S4D). By contrast, the expression of most DNA methyltransferases and demethylases was decreased in blastocysts of rats supplemented with 1.0% methionine (Figure S4D). Additionally, *Dnmt3a* expression showed the strongest positive correlation with the global DNA methylation level (Pearson $r = 0.63$; Figure S4E), implying that *Dnmt3a* might be a main methyltransferase regulating blastocyst methylation. To further study the effect of histone and DNA methylation on blastocysts, embryos were cultured and treated with methionine in the presence or absence of H3K4 and DNA methylation inhibitors. Interestingly, compared with the control group, inhibition of H3K4 methylation caused a significant increase in DNA methylation, while inhibition of DNA methylation led to a rise in H3K4 methylation (Figure S4F), suggesting an antagonistic relationship between DNA methylation and H3K4 methylation in early development of the blastocyst. These results indicate that methionine has an opposite effect on DNA and histone methylation, thus establishing a unique methylation and transcriptional profile in the blastocyst.

(H) The number of implantation sites for mice with zygotes microinjected with IL-5 and a neutralizing anti-IL-5 mAb.

(I) The number of implantation sites of rats injected with saline, IL-5, or a neutralizing anti-IL-5 mAb into the uterine horns.

(J and K) Western blot analysis for IL-5, p65 NF- κ B, and integrin $\alpha\beta\beta$ in the implantation-site tissues of rats injected with saline, IL-5, or a neutralizing anti-IL-5 mAb into the uterine horns.

(L) The number of Th1 and Th2 cells at the maternal-fetal interface in rats injected with saline, IL-5, or a neutralizing anti-IL-5 mAb into the uterine horns.

(M) The number of implantation sites of immunological spontaneous abortion mice fed diets containing different levels of methionine and administered intraperitoneal injections of IL-5, a neutralizing anti-IL-5 mAb, and PBS.

(N and O) Western blot analysis for IL-5, IL-5RA, p65 NF- κ B, and integrin $\alpha\beta\beta$ in the implantation-site tissues of immunological spontaneous abortion mice fed diets containing different levels of methionine and administered intraperitoneal injections of IL-5, a neutralizing anti-IL-5 mAb, and PBS. NP, syngeneic pregnant; AP, allogeneic pregnant.

Data are mean \pm SEM of at least three independent experiments. * $p < 0.05$. See also Figure S3.

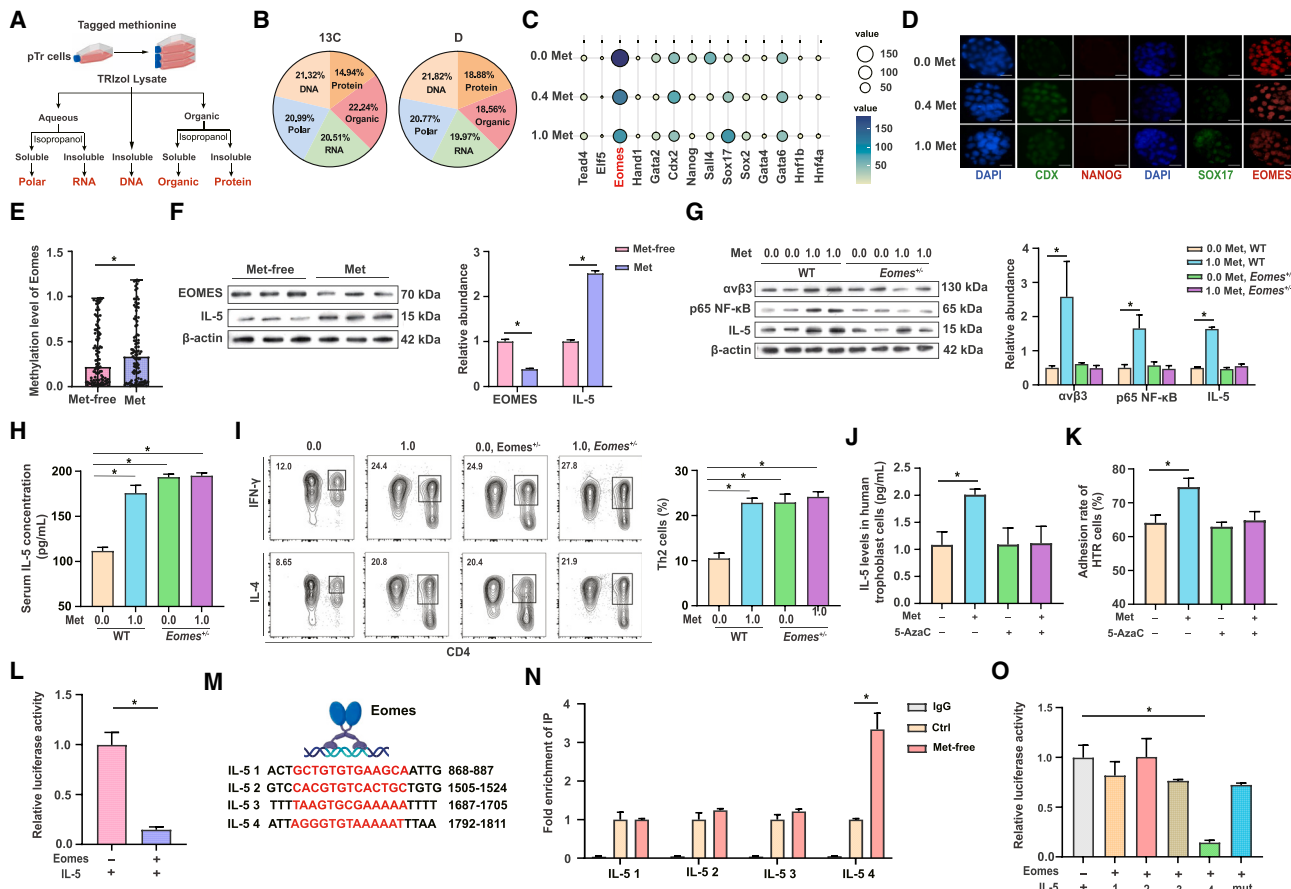


Figure 4. Methionine enhanced IL-5 transcription by regulating methylation of the transcription factor *Eomes*

- (A) Schematic of the process used to fractionate cells into different macromolecular classes based on differential solubility. Material not precipitated from the aqueous phase is referred to as the polar fraction, and material not precipitated from the organic phase is referred to as the non-polar fraction.
 - (B) The relative contributions of methionine carbon-13 and hydrogen-3 to different macromolecular fractions were determined for porcine trophoblast cells.
 - (C) Heatmap showing differentially expressed transcription factors in rat blastocyst.
 - (D) Immunofluorescence staining of CDX, NANOG, SOX17, EOMES, and DAPI in blastocysts of rat fed different methionine diets. Scale bar: 50 μm. CDX2, caudal type homeobox 2; NANOG, NANOG homeobox protein; SOX17, SRY-box transcription factor 17.
 - (E) DNA methylation levels of Eomes in rat blastocyst.
 - (F) Western blot analysis for Eomes and IL-5 in human trophoblast cells treated with methionine.
 - (G) Western blot analysis for p65 NF-κB, integrin αvβ3, and IL-5 in the implantation-site tissues of *Eomes*^{+/−} mice fed different concentrations of methionine during pregnancy.
 - (H) The concentration of serum IL-5 in WT and *Eomes*^{+/−} mice fed methionine.
 - (I) The number of Th2 cells in the maternal-fetal interface of WT and *Eomes*^{+/−} mice fed methionine.
 - (J) IL-5 concentration in human trophoblast cells treated with methionine and the DNA methylation inhibitor 5-azacytidine.
 - (K) The adhesion rate for human trophoblast cells treated with methionine and the DNA methylation inhibitor 5-azacytidine.
 - (L) The relative luciferase activity in human trophoblast cells cotransfected with Eomes and the IL-5 promoter.
 - (M) The four putative GC-rich regions (IL-5 1, 2, 3, and 4) on the IL-5 promoter.
 - (N) The enrichment of EOMES binding IL-5 promoters in human trophoblast cells.
 - (O) The relative luciferase activity in human trophoblast cells cotransfected with Eomes and the IL-5 promoter.
- All data are presented as the mean ± SEM of at least three independent experiments. *p < 0.05. See also Figure S4.

Comparisons of gene expression and promoter methylation in blastocysts showed that >97% of gene promoters were hypermethylated in methionine-deficient blastocysts, resulting in 153 genes or 17% of the corresponding genes being downregulated in methionine-deficient blastocysts compared to the control group. In addition, 25 genes displayed promoter demethylation and were upregulated in methionine-supplemented blastocysts

(Table S2). These genes could be clustered into five groups: regulation of cellular component size, cell morphogenesis involved in differentiation, oxidative phosphorylation, purine ribonucleotide biosynthetic process, and cytokine-cytokine receptor interactions (Figure S4G).

To elucidate the regulatory mechanism of methionine on IL-5, we analyzed the expression of key transcription factors regulating

the differentiation of inner cell mass and trophoblast cells in rat blastocysts fed different methionine diets by transcriptome analysis and immunofluorescence staining. Notably, the expression of *Eomes*, the marker of trophoblast cells, was regulated most dramatically by dietary methionine, showing abundant expression in methionine-deprived blastocysts with a dose-dependent reduction in response to increasing methionine supplementation (Figures 4C and 4D). These results suggest that methionine regulates the transcription of *Eomes*, which may be a critical transcription factor impacting embryonic development. In addition, we conducted bisulfite sequencing PCR and targeted methylation analysis for *Eomes* and *IL-5* in cultured human trophoblast cells in response to methionine. Compared to the methionine-free group, the DNA methylation level of *Eomes* was significantly higher in the methionine-supplemented cells; however, the DNA methylation level of *IL-5* showed no difference (Figure 4E; Table S3). Additionally, the protein expression of EOMES was decreased, while IL-5 expression increased in the methionine-supplemented group (Figure 4F). To clarify the effects of *Eomes* on IL-5 and maternal-fetal immune tolerance, we constructed *Eomes*^{+/-} mice and fed them different concentrations of methionine during pregnancy. In wild-type (WT) mice, the expression of IL-5, p65 NF- κ B, and integrin α v β 3 was reduced when dietary methionine was lacking. However, *Eomes* knockout completely abolished abnormal expressions of IL-5 in response to methionine deficiency (Figure 4G). In addition, the concentration of IL-5 in serum and the number of Th2 cells in the maternal-fetal interface showed similar changes (Figures 4H and 4I). These results were further confirmed in human trophoblast cells, methionine supplementation or *Eomes* knockdown increased the concentration of IL-5 (Figure S4H), the adhesion rate (Figure S4I), and the expression of p65 NF- κ B and integrin α v β 3 (Figure S4J). In addition, we co-caged *Eomes*^{+/-} and *IL-5*^{-/-} mice and detected the IL-5 concentration in serum and the number of implantation sites. In *IL-5*^{+/-} mice, compared to the control group, *Eomes* knockout significantly increased the serum IL-5 concentration, the number of implantation sites, and the expression of p65 NF- κ B and integrin α v β 3 in the implantation-site tissues (Figures S4K-S4M). However, compared to the control group, in *IL-5*^{-/-} mice, both *Eomes* knockout and normal expression led to decreased serum IL-5 levels, implantation site numbers, and the expression of p65 NF- κ B and integrin α v β 3 in the implantation site tissues (Figures S4K-S4M). To further determine whether methionine regulated immune tolerance through methylation modification of *Eomes*, we performed *in vitro* culture experiments of human trophoblast cells. We treated cells with methionine and the DNA methylation inhibitor 5-azacytidine. The results showed that, compared to the control group, methionine supplementation significantly enhanced IL-5 secretion and the embryo adhesion rate (Figures 4J and 4K). However, upon treatment with the DNA methylation inhibitor, neither the secretion of IL-5 nor the embryo adhesion rate of trophoblast cells demonstrated significant differences in the methionine addition or deficiency groups compared to the control group (Figures 4J and 4K). These results clearly indicated that methionine improved maternal-fetal immune tolerance by promoting IL-5 expression through *Eomes*.

To further determine how *Eomes* regulates IL-5, we found that co-transfection of *Eomes* diminished the *IL-5* promoter-driven

luciferase activity, suggesting that *Eomes* inhibits *IL-5* gene transcription (Figure 4L). Because of the presence of four putative *Eomes* binding sites on the *IL-5* promoter (Figure 4M), we sought to determine whether EOMES binds directly to the *IL-5* gene promoter. Specifically, we performed ChIP and dual-luciferase experiments, and the enrichment of EOMES binding following methionine treatment was noted at these regions of IL-5, and it resulted in an approximately 4-fold decrease in gene expression compared to the control group (Figures 4N and 4O). Taken together, these results demonstrate that methionine modulates the expression of *Eomes*, which suppresses IL-5 synthesis by binding to its promoter.

Methionine regulates the expression of EOMES and IL-5 in the placenta

Eomes is initially expressed in the trophectoderm of a blastocyst, which further differentiates into the extra-embryonic ectoderm and placenta.³⁴ To assess the impact of methionine on placental development, we detected the levels of SAM and SAH on days 12, 14, and 18 of pregnancy. The concentrations of SAM were increased in the placenta in the methionine supplementation groups on days 12, 14, and 18 of pregnancy (Figures 5A–5C), while the concentrations of SAH were increased in the placenta in the methionine supplementation groups on day 18 of pregnancy (Figures 5D–5F). Interestingly, we observed a significant decrease in protein expression of EOMES in response to methionine (Figures 5G and 5H). In addition, methionine significantly increased IL-5, IL-5RA, p65 NF- κ B, and integrin α v β 3 expression (Figures 5G and 5H). These data indicate that regulation of *Eomes* by methionine in the blastocyst may continue to influence subsequent placental development.

To better understand how methionine regulates placental development and function, we performed RNA-seq in the placenta of rats fed different levels of methionine. Compared with the control group, 201 genes were downregulated and 104 genes were upregulated by methionine deprivation, while 75 genes were downregulated and 61 genes were upregulated by 1.0% methionine (Figure S5A). Differentially enriched genes are involved in oxygen transport, synthesis of leukotrienes and eoxins, DNA methylation, and cytokine-cytokine receptor interactions (Figure S5B). Of particular interest is that we observed increased expression of genes related to immunomodulation as well as adhesion and recruitment in the methionine-deprived placentae (Figure S5C), suggesting that the immune response is heightened when methionine is deficient, thus impacting maternal-fetal immune tolerance. Indeed, the expression of Th2 cytokines (*IL-5*, *IL-6*, and *IL-10ra*) were reduced in methionine-deficient placentae (Figure S5D). Collectively, these data indicated that methionine has a long-term effect on the regulation of *Eomes* in the blastocyst, influencing IL-5 secretion and placental development and, thus, regulating maternal-fetal immune tolerance.

DISCUSSION

In this study, we tried to improve our understanding of how the regulation of maternal nutrition affects maternal-fetal immune tolerance. We specifically examined the one-carbon nutrient

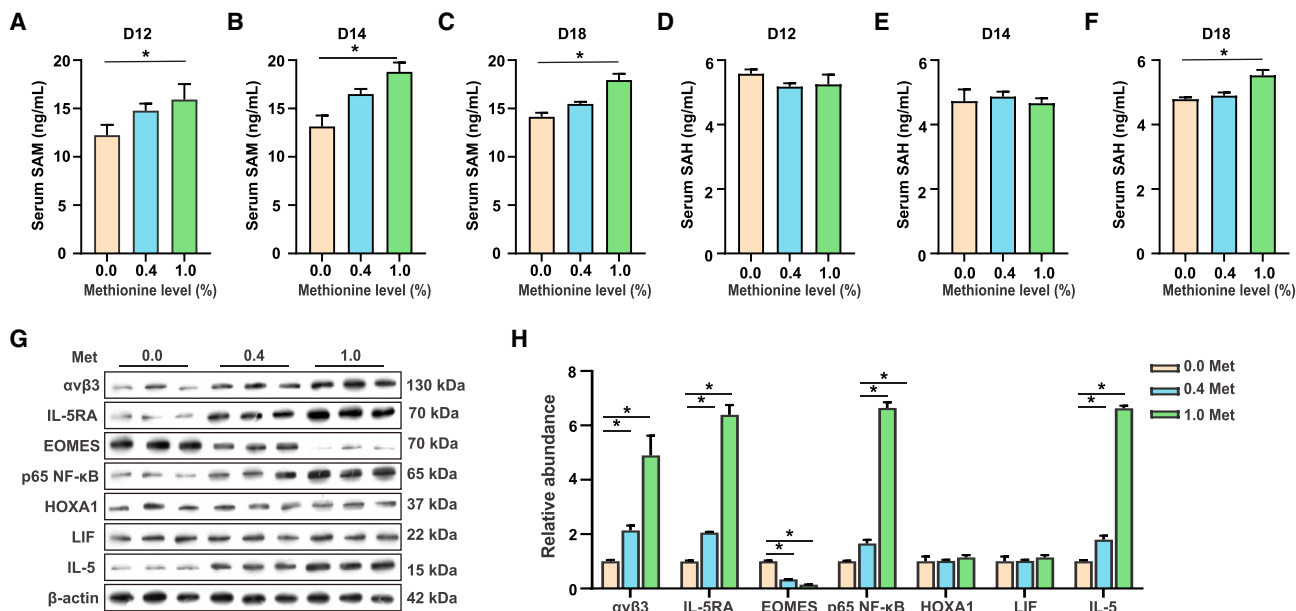


Figure 5. Methionine regulated the expression of EOMES and IL-5 in the placenta

(A–F) The serum concentrations of the methionine metabolites SAM and SAH with different methionine diets on days 12, 14, and 18 of pregnancy. (G–H) Western blot analysis for IL-5RA, IL-5, EOMES, HOXA1, LIF, p65 NF-κB, and integrin $\alpha v\beta 3$ in the placenta of rats fed different concentrations of methionine during pregnancy.

$n = 12$. All data are presented as the mean \pm SEM. * $p < 0.05$. See also Figure S5.

methionine and demonstrated that it improves embryonic development and pregnancy outcomes in rats and pigs through its role in the maintenance of maternal-fetal immune tolerance that is effected via IL-5 secretion. These findings reveal a novel function of methionine and IL-5 in maternal-fetal immune tolerance.

We established an innovative mathematical model that was combined with response surface analysis to study the effects of one-carbon nutrients that are known to be important for embryo implantation. An interesting finding of this analysis was that methionine played a predominant role in embryonic implantation compared with betaine, choline, and folate. Further, we conducted feeding experiments and *in vitro* embryo culture experiments on rats and sows and verified that methionine status during early pregnancy had an impact on embryonic development and pregnancy outcomes. More importantly, our study pointed out that maternal methionine status during pregnancy had a more impressive influence on the fetus than on the mother and even impacted the growth and health of offspring after birth. At present, the focus is largely on folic acid supplementation during pregnancy, and the critical role of methionine has not been recognized. We hope that our findings will draw attention to the importance of this nutrient during pregnancy and that physicians start considering methionine supplementation in pregnant patients.

Histone modifications and DNA methylation are critical in maintaining cell identity and controlling gene expression in early embryos, which undergo re-differentiation from the totipotent embryonic state to various differentiated somatic cell types.^{35–37} Histone modifications are key regulatory events throughout pre-implantation embryogenesis that influence the interactions of

transcriptional regulators with chromatin.^{38,39} Further, DNA methylation is an inheritable type of epigenetic marker that provides the molecular memory required to preserve the transcriptional order during mammalian early embryo development.^{40,41} As a methyl donor, methionine can enhance the methylation levels in a variety of cells. However, research about methionine-mediated regulation of epigenetic programming in embryos is limited. In this study, we performed ultra-low-input native ChIP-seq analysis of H3K4me3, WGBS of DNA methylation, and association analysis of blastocyst transcriptomes to uncover the influence of methionine on methylation profiles during blastocyst development. Our results showed that Dnmt3a was the most significant methyltransferase that displayed a positive correlation with the global DNA methylation level in response to methionine treatment of blastocysts. Surprisingly, we noticed that methionine supplementation increased the level of H3K4me3 but decreased the global DNA methylation level in rat blastocysts, which is different from the regulatory effects of methionine in cancer cells. Consistent with the whole-genome methylation status, the expression of H3K4 and DNA methyltransferases and demethylases was significantly regulated in response to methionine treatment. Specifically, most DNA methyltransferases (Dnmt3a, Dnmt3b, and Dnmt3l) showed higher expression in response to methionine deprivation, while H3K4 methyltransferases (Kmt2a, Kmt2b, Kmt2c, Kmt2d, and Kmt2e) showed higher expression in response to methionine supplementation. These expression patterns were consistent with the methylation status of blastocysts. In addition, immunofluorescence staining experiments in rat blastocysts demonstrated that methionine induced an increase in the level of H3K4me3

and a decrease in the level of DNA methylation. Altogether, these findings are indicative of the interactive effects of H3K4 and DNA methylation on embryo development and the modulatory role of methionine in these effects.

The bulk levels, positional locations (with regard to promoter, enhancer, and repressor binding), and geometrical properties of methylation modifications have been shown to contribute to a number of developmental processes.⁴² DNA or histone methylation control the selection of promoters by affecting the binding of methylated binding proteins or transcription factors.^{34,43} In the context of pregnancy, our study revealed significant changes in the DNA methylation status of *Eomes* in response to methionine levels in the blastocysts and placenta. Of particular note is that methionine had an opposite effect on the methylation level of *Eomes* and global DNA. This may be due to the complex regulatory mechanisms of methylation, which involves multiple factors, such as the activity of DNA methyltransferases, the status of histone methylation and acetylation, phosphorylation, and the interplay of these epigenetic modifications.⁴⁴ Expression of *Eomes*, which is a paralog of the T-bet transcription family, was first detected in the trophoblast lineage and found to start in the trophectoderm of the blastocyst, which forms the fetal portion of the placenta.^{6,45} During pregnancy, trophoblasts express and secrete a battery of cytokines and chemokines to sustain maternal-fetal immune tolerance, such as IL-34 and IL-35.⁴⁶ This implies that the expression of *Eomes* in the blastocysts and placenta may be related to maternal-fetal immunity. In line with this notion, studies have found that *Eomes* identifies thymic precursors of self-specific memory-phenotype CD8⁺ T cells.⁴⁷ Further, the overexpression of *Eomes* in activated CD8⁺ T cells leads to impaired effector functions and is directly involved in the regulation of T cell exhaustion by B7S1 signals,^{48,49} resulting in Th1/Th2 imbalance and embryonic implantation failure.^{50–55} However, it is unclear whether *Eomes* can directly regulate cytokine secretion in embryos and, thus, influence embryonic implantation. In this study, we constructed *Eomes*^{+/-} mice and performed *Eomes* small interfering RNA interference experiments on human and porcine trophoblast cells, and our results showed that methionine modulated the IL-5 levels in the serum and embryos via the transcription factor *Eomes*, which activated the NF-κB pathway and enhanced integrin αvβ3 expression. Through ChIP-qPCR and dual-luciferase reporter gene experiments, we verified that *Eomes* binds directly to the IL-5 promoter regions to inhibit IL-5 transcription, while methionine supplementation prevents the binding of *Eomes* to IL-5 to improve embryonic immunity.

In summary, our study has elucidated the unique regulatory network established by methionine in embryos and the molecular mechanism by which methionine enhanced early embryonic development. Our findings advance the current knowledge of how methionine regulates early embryonic immunity and lay the basis for nutritional strategies involving methionine supplementation for successful pregnancy by promoting maternal-fetal immune tolerance and endometrial receptivity.

Limitations of the study

Our study revealed that methionine promotes the secretion of IL-5, which enhances embryonic implantation. As a result, we

dedicated our attention to the IL-5 cytokine and conducted a series of experiments that included microinjections into embryos, injections into the uterine horns, and intraperitoneal injections of IL-5 and IL-5 mAbs, along with the use of IL-5 knockout mice. These results underscored the pivotal role of IL-5 in endometrial receptivity and maternal-fetal immune tolerance. However, the role of IL-5 in human maternal-fetal immunity remains to be confirmed and necessitates further validation with a larger set of clinical samples. Moreover, our study did not delve into the potential synergistic effects that could result from the interactions among various cytokines. Furthermore, we discovered that methionine decreases the overall DNA methylation levels in blastocysts and increases the global levels of H3K4me3 methylation. The complex interplay among epigenetic modifications was not deeply explored.

RESOURCE AVAILABILITY

Lead contact

Further information and requests for resources and reagents should be directed to and will be fulfilled by the lead contact, Xiangfang Zeng (zengxf@cau.edu.cn).

Materials availability

This study did not generate new reagents or mouse lines.

Data and code availability

- All sequencing data for this study are available from the NCBI database (Accession number: PRJNA1061084 and PRJNA1061078).
- This study does not report original code.
- Any additional information required to reanalyze the data reported in this study is available from the [lead contact](#) upon request.

ACKNOWLEDGMENTS

This study was supported by the National Natural Science Foundation of China (grants 32425052 and 32172747), the Beijing Higher Education Outstanding Young Scientists Project, and the Beijing Innovation Consortium of Livestock Research System (BAIC05-2024).

AUTHOR CONTRIBUTIONS

Conceptualization, S.C., X.Z., and S.Q.; methodology, S.C., B.X., X.W., H.Y., and Z.Z.; investigation, S.C., X.Z., S.L., Z.Z., B.X., Y.Z., and X.W.; visualization, S.C. and X.Z.; supervision, X.Z. and S.Q.; writing – original draft, S.C.; writing – review & editing, S.C. and X.Z.

DECLARATION OF INTERESTS

The authors declare no competing interests.

STAR METHODS

Detailed methods are provided in the online version of this paper and include the following:

- KEY RESOURCES TABLE
- EXPERIMENTAL MODEL AND STUDY PARTICIPANT DETAILS
 - Animals
 - Cell lines and cell culture
- METHOD DETAILS
 - Response surface
 - Immunofluorescence staining
 - Flow cytometry

- Microinjection
 - Cell adhesion assay
 - Cell fractionation
 - Blastocyst samples collection and preparation
 - WGBS library and analysis
 - RNA preparation and sequencing
 - Ultra-low-input native ChIP-seq of H3K4me3
 - Serum methionine metabolism measurement
 - Cytokines detection
 - Placenta collection
 - Western blotting analysis
 - Transfections
 - Plasmid construction and dual-luciferase reporter assays
 - Chromatin immunoprecipitation
- QUANTIFICATION AND STATISTICAL ANALYSIS

SUPPLEMENTAL INFORMATION

Supplemental information can be found online at <https://doi.org/10.1016/j.celrep.2025.115291>.

Received: January 30, 2024

Revised: July 25, 2024

Accepted: January 17, 2025

Published: February 11, 2025

REFERENCES

1. Aghaeepour, N., Ganio, E.A., Mcilwain, D., Tsai, A.S., Tingle, M., Van Gasen, S., Gaudilliere, D.K., Baca, Q., Mcneil, L., Okada, R., et al. (2017). An immune clock of human pregnancy. *Sci. Immunol.* 2, eaan2946.
2. Billingham, R.E., Brent, L., and Medawar, P.B. (1953). "Actively acquired tolerance" of foreign cells. *Nature* 172, 603–606.
3. Mor, G., and Cardenas, I. (2010). The immune system in pregnancy: a unique complexity. *Am. J. Reprod. Immunol.* 63, 425–433.
4. Liu, J., Hao, S., Chen, X., Zhao, H., Du, L., Ren, H., Wang, C., and Mao, H. (2019). Human placental trophoblast cells contribute to maternal-fetal tolerance through expressing IL-35 and mediating iTR35 conversion. *Nat. Commun.* 10, 4601.
5. Wang, W., Sung, N., Gilman-Sachs, A., and Kwak-Kim, J. (2020). T helper (Th) cell profiles in pregnancy and recurrent pregnancy losses: Th1/Th2/Th9/Th17/Th22/Tfh cells. *Front. Immunol.* 11, 2025.
6. Wang, X.Q., and Li, D.J. (2020). The mechanisms by which trophoblast-derived molecules induce maternal-fetal immune tolerance. *Cell. Mol. Immunol.* 17, 1204–1207.
7. Pauwels, S., Ghosh, M., Duca, R.C., Bekaert, B., Freson, K., Huybrechts, I., A S Langie, S., Koppen, G., Devlieger, R., and Godderis, L. (2017). Dietary and supplemental maternal methyl-group donor intake and cord blood DNA methylation. *Epigenetics* 12, 1–10.
8. Chen, M., Zhang, B., Cai, S., Zeng, X., Ye, Q., Mao, X., Zhang, S., Zeng, X., Ye, C., and Qiao, S. (2019). Metabolic disorder of amino acids, fatty acids and purines reflects the decreases in oocyte quality and potential in sows. *J. Proteonomics* 200, 134–143.
9. Zhao, J., Whyte, J., and Prather, R.S. (2010). Effect of epigenetic regulation during swine embryogenesis and on cloning by nuclear transfer. *Cell Tissue Res.* 341, 13–21.
10. Kirke, P.N., Molloy, A.M., Daly, L.E., Burke, H., Weir, D.G., and Scott, J.M. (1993). Maternal plasma folate and vitamin B12 are independent risk factors for neural tube defects. *Q. J. Med.* 86, 703–708.
11. Häberg, S.E., London, S.J., Stigum, H., Nafstad, P., and Nystad, W. (2009). Folic acid supplements in pregnancy and early childhood respiratory health. *Arch. Dis. Child.* 94, 180–184.
12. George, L., Mills, J.L., Johansson, A.L.V., Nordmark, A., Olander, B., Granath, F., and Cnattingius, S. (2002). Plasma folate levels and risk of spontaneous abortion. *JAMA* 288, 1867–1873.
13. van Beynum, I.M., Kapusta, L., Bakker, M.K., den Heijer, M., Blom, H.J., and de Walle, H.E.K. (2010). Protective effect of periconceptional folic acid supplements on the risk of congenital heart defects: A registry-based case-control study in the northern Netherlands. *Eur. Heart J.* 31, 464–471.
14. Boeke, C.E., Gillman, M.W., Hughes, M.D., Rifas-Shiman, S.L., Villamor, E., and Oken, E. (2013). Choline intake during pregnancy and child cognition at age 7 years. *Am. J. Epidemiol.* 177, 1338–1347.
15. Su, X., Wellen, K.E., and Rabinowitz, J.D. (2016). Metabolic control of methylation and acetylation. *Curr. Opin. Chem. Biol.* 30, 52–60.
16. Cai, S., Ye, Q., Zeng, X., Yang, G., Ye, C., Chen, M., Yu, H., Wang, Y., Wang, G., Huang, S., et al. (2021). CBS and MAT2A improve methionine-mediated DNA synthesis through SAMTOR/mTORC1/S6K1/CAD pathway during embryo implantation. *Cell Prolif.* 54, e12950.
17. Cai, S., Quan, S., Yang, G., Zeng, X., Wang, X., Ye, C., Li, H., Wang, G., Zeng, X., and Qiao, S. (2023). DDIT3 regulates key enzymes in the methionine cycle and flux during embryonic development. *J. Nutr. Biochem.* 111, 109176.
18. Cai, S., Quan, S., Yang, G., Chen, M., Ye, Q., Wang, G., Yu, H., Wang, Y., Qiao, S., and Zeng, X. (2021). Nutritional status impacts epigenetic regulation in early embryo development: A scoping review. *Adv. Nutr.* 12, 1877–1892.
19. Fang, L., Hao, Y., Yu, H., Gu, X., Peng, Q., Zhuo, H., Li, Y., Liu, Z., Wang, J., Chen, Y., et al. (2023). Methionine restriction promotes cGAS activation and chromatin untethering through demethylation to enhance antitumor immunity. *Cancer Cell* 41, 1118–1133.e12.
20. Gao, X., Sanderson, S.M., Dai, Z., Reid, M.A., Cooper, D.E., Lu, M., Richie, J.P., Ciccarella, A., Calcagnotto, A., Mikhael, P.G., et al. (2019). Dietary methionine influences therapy in mouse cancer models and alters human metabolism. *Nature* 572, 397–401.
21. Sanderson, S.M., Gao, X., Dai, Z., and Locasale, J.W. (2019). Methionine metabolism in health and cancer: a nexus of diet and precision medicine. *Nat. Rev. Cancer* 19, 625–637.
22. Sharma, A., Blériot, C., Currenti, J., and Ginhoux, F. (2022). Oncofetal reprogramming in tumour development and progression. *Nat. Rev. Cancer* 22, 593–602.
23. Wang, Z., Yip, L.Y., Lee, J.H.J., Wu, Z., Chew, H.Y., Chong, P.K.W., Teo, C.C., Ang, H.Y.K., Peh, K.L.E., Yuan, J., et al. (2019). Methionine is a metabolic dependency of tumor-initiating cells. *Nat. Med.* 25, 825–837.
24. Bian, Y., Li, W., Kremer, D.M., Sajjakulnukit, P., Li, S., Crespo, J., Nwosu, Z.C., Zhang, L., Czerwonka, A., Pawlowska, A., et al. (2020). Cancer SLC43A2 alters T cell methionine metabolism and histone methylation. *Nature* 585, 277–282.
25. Hung, M.H., Lee, J.S., Ma, C., Diggs, L.P., Heinrich, S., Chang, C.W., Ma, L., Forges, M., Budhu, A., Chaisaingmongkol, J., et al. (2021). Tumor methionine metabolism drives T-cell exhaustion in hepatocellular carcinoma. *Nat. Commun.* 12, 1455.
26. Pandit, M., Kil, Y.S., Ahn, J.H., Pokhrel, R.H., Gu, Y., Mishra, S., Han, Y., Ouh, Y.T., Kang, B., Jeong, M.S., et al. (2023). Methionine consumption by cancer cells drives a progressive upregulation of PD-1 expression in CD4 T cells. *Nat. Commun.* 14, 2593.
27. Tzukerman, M., Rosenberg, T., Ravel, Y., Reiter, I., Coleman, R., and Skorecki, K. (2003). An experimental platform for studying growth and invasiveness of tumor cells within teratomas derived from human embryonic stem cells. *Proc. Natl. Acad. Sci. USA* 100, 13507–13512.
28. Hanahan, D., and Weinberg, R.A. (2011). Hallmarks of cancer: the next generation. *Cell* 144, 646–674.
29. Solon-Biet, S.M., Walters, K.A., Simanainen, U.K., McMahon, A.C., Ruohonen, K., Ballard, J.W.O., Raubenheimer, D., Handelman, D.J., Le Couet, D.G., and Simpson, S.J. (2015). Macronutrient balance, reproductive

- function, and lifespan in aging mice. *Proc. Natl. Acad. Sci. USA* **112**, 3481–3486.
30. Solon-Biet, S.M., McMahon, A.C., Ballard, J.W.O., Ruohonen, K., Wu, L.E., Cogger, V.C., Warren, A., Huang, X., Pichaud, N., Melvin, R.G., et al. (2014). The ratio of macronutrients, not caloric intake, dictates cardiometabolic health, aging, and longevity in ad libitum-fed mice. *Cell Metabol.* **19**, 418–430.
 31. Lu, S.C. (2000). S-Adenosylmethionine. *Int. J. Biochem. Cell Biol.* **32**, 391–395.
 32. van der Put, N.M., van Straaten, H.W., Trijbels, F.J., and Blom, H.J. (2001). Folate, homocysteine and neural tube defects: an overview. *Exp. Biol. Med.* **226**, 243–270.
 33. Hosios, A.M., Hecht, V.C., Danai, L.V., Johnson, M.O., Rathmell, J.C., Steinhauser, M.L., Manalis, S.R., and Vander Heiden, M.G. (2016). Amino acids rather than glucose account for the majority of cell mass in proliferating mammalian cells. *Dev. Cell* **36**, 540–549.
 34. Russ, A.P., Wattler, S., Colledge, W.H., Aparicio, S.A., Carlton, M.B., Pearce, J.J., Barton, S.C., Surani, M.A., Ryan, K., Nehls, M.C., et al. (2000). Eomesodermin is required for mouse trophoblast development and mesoderm formation. *Nature* **404**, 95–99.
 35. Xu, R., Li, C., Liu, X., and Gao, S. (2021). Insights into epigenetic patterns in mammalian early embryos. *Protein Cell* **12**, 7–28.
 36. Smith, Z.D., Chan, M.M., Humm, K.C., Karnik, R., Mekhoubad, S., Regev, A., Eggan, K., and Meissner, A. (2014). DNA methylation dynamics of the human preimplantation embryo. *Nature* **511**, 611–615.
 37. Tamada, H., and Kikyo, N. (2004). Nuclear reprogramming in mammalian somatic cell nuclear cloning. *Cytogenet. Genome Res.* **105**, 285–291.
 38. Skvortsova, K., Iovino, N., and Bogdanović, O. (2018). Functions and mechanisms of epigenetic inheritance in animals. *Nat. Rev. Mol. Cell Biol.* **19**, 774–790.
 39. Wu, J., Xu, J., Liu, B., Yao, G., Wang, P., Lin, Z., Huang, B., Wang, X., Li, T., Shi, S., et al. (2018). Chromatin analysis in human early development reveals epigenetic transition during ZGA. *Nature* **557**, 256–260.
 40. Branco, M.R., King, M., Perez-Garcia, V., Bogutz, A.B., Caley, M., Fineberg, E., Lefebvre, L., Cook, S.J., Dean, W., Hemberger, M., and Reik, W. (2016). Maternal DNA methylation regulates early trophoblast development. *Dev. Cell* **36**, 152–163.
 41. Okano, M., Bell, D.W., Haber, D.A., and Li, E. (1999). DNA methyltransferases Dnmt3a and Dnmt3b are essential for de novo methylation and mammalian development. *Cell* **99**, 247–257.
 42. Prather, R.S., Ross, J.W., Isom, S.C., and Green, J.A. (2009). Transcriptional, post-transcriptional and epigenetic control of porcine oocyte maturation and embryogenesis. *Soc. Reprod. Fertil. Suppl.* **66**, 165–176.
 43. Jones, P.A. (2012). Functions of DNA methylation: islands, start sites, gene bodies and beyond. *Nat. Rev. Genet.* **13**, 484–492.
 44. Waterland, R.A. (2006). Assessing the effects of high methionine intake on DNA methylation. *J. Nutr.* **136**, 1706S–1710S.
 45. Robertson, E.J., Arnold, S.J., Costello, I., Pimeisl, I., Dräger, S., and Bikoff, E.K. (2011). The T-box transcription factor Eomesodermin acts upstream of Mesp1 to specify cardiac mesoderm during mouse gastrulation. *Nat. Cell Biol.* **13**, 1084–1091.
 46. Miller, C.H., Klawon, D.E.J., Zeng, S., Lee, V., Socci, N.D., and Savage, P.A. (2020). Eomes identifies thymic precursors of self-specific memory-phenotype CD8⁺ T cells. *Nat. Immunol.* **21**, 567–577.
 47. Li, J., Lee, Y., Li, Y., Jiang, Y., Lu, H., Zang, W., Zhao, X., Liu, L., Chen, Y., Tan, H., et al. (2018). Co-inhibitory molecule B7 superfamily member 1 expressed by tumor-infiltrating myeloid cells induces dysfunction of anti-tumor CD8⁺ T Cells. *Immunity* **48**, 773–786.e5.
 48. Buggert, M., Tauriainen, J., Yamamoto, T., Frederiksen, J., Ivarsson, M.A., Michaélsson, J., Lund, O., Hejdeman, B., Jansson, M., Sönnernborg, A., et al. (2014). T-bet and Eomes are differentially linked to the exhausted phenotype of CD8⁺ T cells in HIV infection. *PLoS Pathog.* **10**, e1004251.
 49. Kuroda, K., Nakagawa, K., Horikawa, T., Moriyama, A., Ojiro, Y., Takamizawa, S., Ochiai, A., Matsumura, Y., Ikemoto, Y., Yamaguchi, K., and Sugiyama, R. (2021). Increasing number of implantation failures and pregnancy losses associated with elevated Th1/Th2 cell ratio. *Am. J. Reprod. Immunol.* **86**, e13429.
 50. Csabai, T., Pallinger, E., Kovacs, A.F., Miko, E., Bognar, Z., and Szekeres-Bartho, J. (2020). Altered immune response and implantation failure in progesterone-induced blocking factor-deficient mice. *Front. Immunol.* **11**, 349.
 51. Liang, P.Y., Yin, B., Cai, J., Hu, X.D., Song, C., Wu, T.H., Zhao, J., Li, G.G., and Zeng, Y. (2015). Increased circulating Th1/Th2 ratios but not other lymphocyte subsets during controlled ovarian stimulation are linked to subsequent implantation failure after transfer of in vitro fertilized embryos. *Am. J. Reprod. Immunol.* **73**, 12–21.
 52. Nakagawa, K., Kwak-Kim, J., Ota, K., Kuroda, K., Hisano, M., Sugiyama, R., and Yamaguchi, K. (2015). Immunosuppression with tacrolimus improved reproductive outcome of women with repeated implantation failure and elevated peripheral blood TH1/TH2 cell ratios. *Am. J. Reprod. Immunol.* **73**, 353–361.
 53. Lan, Y., Li, Y., Yang, X., Lei, L., Liang, Y., and Wang, S. (2021). Progesterone-induced blocking factor-mediated Th1/Th2 balance correlates with fetal arrest in women who underwent in vitro fertilization and embryo transfer. *Clin. Immunol.* **232**, 108858.
 54. Meng, T.G., Guo, J.N., Zhu, L., Yin, Y., Wang, F., Han, Z.M., Lei, L., Ma, X.S., Xue, Y., Yue, W., et al. (2023). NLRP14 safeguards calcium homeostasis via regulating the K27 ubiquitination of Nclx in oocyte-to-embryo transition. *Adv. Sci.* **10**, e2301940.
 55. Brind Amour, J., Liu, S., Hudson, M., Chen, C., Karimi, M.M., and Lorincz, M.C. (2015). An ultra-low-input native ChIP-seq protocol for genome-wide profiling of rare cell populations. *Nat. Commun.* **6**, 6033.
 56. Fu, B., Li, X., Sun, R., Tong, X., Ling, B., Tian, Z., and Wei, H. (2013). Natural killer cells promote immune tolerance by regulating inflammatory T_H17 cells at the human maternal-fetal interface. *Proc. Natl. Acad. Sci. USA* **110**, E231–E240.

STAR★METHODS

KEY RESOURCES TABLE

REAGENT or RESOURCE	SOURCE	IDENTIFIER
Antibodies		
5mC	Sigma-Aldrich	Cat# MABE1081; RRID: AB_3675813
5hmC	Sigma-Aldrich	Cat# MABE317; RRID: AB_3675812
β-actin	Proteintech	Cat# 20536-1-AP; RRID:AB_10700003
EOMES	Proteintech	Cat# 28316-1-AP; RRID:AB_2881110
H3K4me3	Sigma-Aldrich	Cat# 04-745; RRID:AB_1163444
H3K9me3	Sigma-Aldrich	Cat# 07-442; RRID:AB_310620
H3K27me3	Sigma-Aldrich	Cat# 07-449; RRID:AB_310624
HOXA1	Bioss	Cat# bs-17361R; RRID:AB_3675811
IL-5	Invitrogen	Cat# 14-7052-85; RRID:AB_468421
IL-5RA	Proteintech	Cat# 12655-1-AP; RRID:AB_2127342
integrin αvβ3	Bioss	Cat# bs-1310R; RRID:AB_10854294
LIF	Proteintech	Cat# 26757-1-AP; RRID:AB_2880624
NF-κB p65	Proteintech	Cat# 66535-1-Ig; RRID:AB_2881898
p38 MAPK	Bioss	Cat# bs-0637R; RRID:AB_10856281
CD45	BD Biosciences	Cat# 564279; RRID:AB_2651134
IL-17	BD Biosciences	Cat# 564171; RRID:AB_2738642
IL-4	BD Biosciences	Cat# 564005; RRID:AB_2738537
CD4	BD Biosciences	Cat# 563151; RRID:AB_2687549
CD3	BD Biosciences	Cat# 563024; RRID:AB_2737959
CD68	BD Biosciences	Cat# 566388; RRID:AB_2744447
CD25	BD Biosciences	Cat# 564424; RRID:AB_2738803
CD163	BioLegend	Cat# 155305; RRID:AB_2814059
CD86	BD Biosciences	Cat# 567592; RRID:AB_2916657
IFN- γ	BD Biosciences	Cat# 554412; RRID:AB_395376
Foxp3	BD Biosciences	Cat# 560401; RRID:AB_1645201
Chemicals, peptides, and recombinant proteins		
Methionine used in feed	CJ International Trading Co., Ltd.	N/A
RPMI 1640	Gibco	Cat# 11875093
DMEM/F12	Gibco	Cat# 11320033
Cell Activation Cocktail	BD Biosciences	Cat# 550583
Per-meabilized with intracellular fixation & permeabilization buffer set	BD Biosciences	Cat# 562574
Carboxyfluorescein succinimidyl ester	Invitrogen	Cat# C1157
L-methionine-1-13C-(methyl-D3)	Sigma-Aldrich	Cat# 660876
RIPA lysis	Huaxingbio	Cat# HX1862-2
Lipofectamine 3000	Invitrogen	Cat# L3000150
pRL-TK	Promega	Cat# E2241
Rabbit IgG	Proteintech	Cat# 30000-0-AP
1.5M Tris-HCl pH 8.8, 0.4%SDS	Huaxingbio	Cat# HX1871
1M Tris-HCl pH 6.8, 0.4%SDS	Huaxingbio	Cat# HX1870
DAPI	AATBioquest	Cat#17507
Penicillin/Streptomycin	Sigma-Aldrich	Cat#P4333
Fetal bovine serum	Sigma-Aldrich	Cat#F7524

(Continued on next page)

Continued

REAGENT or RESOURCE	SOURCE	IDENTIFIER
Stain buffer	BD Biosciences	Cat# 554656
Brilliant stain buffer plus	BD Biosciences	Cat# 566385
Critical commercial assays		
NEBNext® Ultra II DNA kit	New England Biolabs	Cat# E7645S
ChIP Assay Kit	Beyotime	Cat# P2080S
PrimeScript™ RT reagent Kit with gDNA Eraser	Takara	Cat# RR047A
RNAiso Plus	Takara	Cat# 9108
Pierce™ BCA Protein Assay Kit	Thermo Scientific	Cat# 23227
Dual-Luciferase Reporter Assay System	Promega	Cat# E1910
Deposited data		
Raw data of rat blastocysts DNA methylation and H3K4 methylation	This study	(https://www.ncbi.nlm.nih.gov/bioproject/) NCBI-BioProject: PRJNA1061084
Raw data of rat blastocysts transcriptome	This study	(https://www.ncbi.nlm.nih.gov/bioproject/) NCBI-BioProject: PRJNA1061078
Experimental models: Cell lines		
Ishikawa cells	Pricella Life Science & Technology Co., Ltd.	Cat# CP-H058
HTR cells	Pricella Life Science & Technology Co., Ltd.	Cat# CL-0765
pTr cells	Zhenlong Wu Laboratory	N/A
PEEC	ATCC	N/A
Experimental models: Organisms/strains		
Sprague-Dawley rats	Huafukang Bioscience Co., Inc	N/A
ICR mice	Huafukang Bioscience Co., Inc	N/A
C57BL/6J	Cyagen Bioscience Co., Inc	N/A
CBA/J	Cyagen Bioscience Co., Inc	N/A
DBA/2J	Cyagen Bioscience Co., Inc	N/A
Oligonucleotides		
qPCRprimers, see Table S2	This paper	N/A
Software and algorithms		
GraphPad Prism 10	GraphPad	N/A
ImageJ	National Institutes of Health	N/A
Design-Expert 10.0.7	Design-Expert	N/A
FlowJo, Version 10.8.1	Ashland,OR:Becton, Dickinson and Company	N/A

EXPERIMENTAL MODEL AND STUDY PARTICIPANT DETAILS

Animals

All murine were housed three per cage in a specific pathogen-free animal room under a controlled environment (23°C and 12 h light: 12 h dark photoperiod, with lights on at 0600). Pregnancy was induced by co-caging overnight, and the presence of spermatozoa in the vaginal smear was defined as day 1 of pregnancy.

A total of 120 (Landrace × Large white) crossbred sows were randomly divided into three groups, which were fed diets supplemented with 0, 0.2% and 0.4% methionine, respectively. Diets met the nutritional requirements of pregnant sows (GB/T 39235-2020 Nutritional Requirements for Swine). All sows were housed in restricted pens (2.2 m × 0.65 m) and were fed at 0600 and 1600. The methionine addition in diets was kept for 28 days from day 1 to day 28 of pregnancy and then fed the same diet until delivery. Serum was collected on day 28 of pregnancy, and the reproductive performance were recorded. The samples were stored in at -80°C. All procedures were approved by China Agricultural University Animal Care and Use Committee (AW21804202-1-2).

Cell lines and cell culture

Ishikawa, HTR and PEEC cells were cultured in RPMI 1640 medium supplemented with 10% FBS, while pTr cells were maintained in DMEM/F12 supplemented with 10% FBS and 1% ITS. The cells were maintained at 37°C in a humidified atmosphere with 5% CO₂.

METHOD DETAILS

Response surface

A total of 220 pregnancy rats were provided *ad libitum* access to water and one of 22 experimental diets varying in methionine, folate, choline, and betaine content (Table S4). On day 7 of pregnancy, all rats were killed. The number of implantation sites, serum SAM and SAH were measured and analyzed as the response.

Immunofluorescence staining

After removing the zona pellucida with acidic operating fluid, rat embryos were fixed in fixative solution for 40 min at room temperature, followed by permeabilization in 1% Triton X-100 for 20 min at room temperature. Embryos were then blocked-in blocking solution consisting of 1% bovine serum albumin in phosphate-buffered saline (PBS) for 1 h at room temperature after three washes in washing solution (0.1% Tween 20, 0.01% Triton X-100 in PBS). Antibody incubation was performed overnight at 4°C. The next day, the embryos were washed in washing solution and incubated with secondary antibodies for 1 h at room temperature. After staining with DAPI, the embryos were washed in washing solution. Embryo imaging was performed using an inverted microscope.

Flow cytometry

Cells were harvested and stained for cell-surface markers with antibodies or their specific isotype controls. For the intracellular staining, cells were first pre-incubated with Cell Activation Cocktail, and then fixed and permeabilized with intracellular fixation & permeabilization buffer set according to the manufacturer's instructions. Flow cytometry detection were performed using BD LSR II/LSRFortessa in the Institute for Immunology, Tsinghua University. Data analysis was performed according to the previous research [56] using Flow Jo V10.8.1.

Microinjection

Zygote-stage embryos were collected and were placed in 150 µg/mL hyaluronidase to digest the outer granule cells. Then, microinjection was performed using a FemtoJet 4i microinjector and E LIPSE Ti micromanipulators. For injection, a glass capillary Femtotip was loaded with 2 µL liquid using a Microloader, and the solution was injected into cytoplasm. The injection conditions consisted of an injection pressure of 250 hPa, compensation pressure of 60 hPa, and injection time of 0.7 s. Immediately after microinjection, embryos were cultured in KSOM medium at 37°C in 5% CO₂.

Cell adhesion assay

Embryo adhesion was performed as previously described.¹⁶ Briefly, human and porcine trophoblast cells were grown on 6-well plates. Trophoblast cells were stained with carboxyfluorescein succinimidyl ester for 1 h before the adhesion assay. The stained cells were plated into endometrial cell monolayers in trophoblast cell culture medium. After 1 h, unattached trophoblast cells were removed, and the attached cells were gently washed with PBS 3 times. The cells were then photographed under a fluorescence microscope or analyzed using flow cytometry. An equal amount of stained trophoblastic cells was plated in 3 blank wells. The adhesion rate was calculated as the percentage of attached trophoblastic cells. All experiments were replicated 3 times.

Cell fractionation

pTr cells were maintained in DMEM/F12 supplemented with 10% FBS and 1% ITS. After reaching 80%–90% confluence, the cells were starved in a customized methionine-free medium overnight. Then, cells were treated with 0.5 mM L-methionine-1-¹³C-(methyl-D₃) for 24 h and collected for cell fractionation.

Cells were lysed using the TRIzol reagent. RNA, DNA, and protein were extracted according to the manufacturer's instructions. In brief, following initial lysis, insoluble material was considered to be DNA. RNA was precipitated from the aqueous phase, and the remaining soluble material was termed the "polar fraction". Protein was precipitated from the organic phase, and the remaining soluble material was termed the "non-polar fraction". After freeze-drying, an isotope mass spectrometer was used to determine the stable isotope profiles of each component.

Blastocyst samples collection and preparation

A total of 30 pregnant rats were assigned randomly into three dietary groups with methionine levels at 0, 0.4%, and 1.0%. On day 5 of pregnancy, all rats were anesthetized and blastocysts were obtained by aspirator tube assembly with a micromanipulator. All blastocysts were assigned into three samples per group, snap-frozen with liquid nitrogen, and stored at –80°C.

WGBS library and analysis

Library concentration was quantified by Qubit 3.0 Fluorometer, and K5500 spectrophotometer was used for the purity. The volume of the combined gDNA sample and unmethylated lambda DNA control was adjusted to a total of 80 µL using 1x TE and fragment the DNA to 300 bp. Blunt-ended fragments were created by filling in or chewing back 3' and 5' overhangs. Phosphorylation of the 5' ends ensured the fragments were suitable for ligation. After dA-Tailing, a single A overhang enabled ligation to adaptors with single T overhangs. Methylated adaptor containing sequences required downstream in the sequencing workflow were ligated to the dA-tailing

fragment. 2% agarose gel selected the fragment 350–500 bp. The bisulfite conversion technique involved treating DNA with bisulfite, which converted unmethylated cytosines into uracil. Methylated cytosines remain unchanged during the treatment. The uracil-binding pocket of KAPA HiFi DNA Polymerase had been inactivated, enabling amplification of uracil-containing DNA. The WGBS library was sequenced on Illumina Hiseq X10 sequencers as paired-end 150 bp reads.

Raw data were stored in FASTQ format, including the base sequence and corresponding quality information. To obtain clean data, adaptor-polluted reads, low-quality reads, and reads with over 10% Ns were removed by in-house script. Clean reads were mapped to reference genome by Bismark and only uniquely mapped reads were retained. Cytosines were considered as methylated based on the binomial test followed by Benjamini-Hochberg false discovery rate correction. The methylation level of a single cytosine was calculated as $mC/(mC + umC)$, where the mC is the number of methylated reads and umC is the number of unmethylated reads. The methylation level of a region was defined as the mean methylation level of cytosines in that defined region. Differential methylated cytosines (DMCs) and Differential methylated regions (DMRs) were called by DSS software with default parameters.

RNA preparation and sequencing

Total RNA was obtained using TRIzol reagent following the standard extraction protocol. The quality and concentration of RNA were determined using a NanoPhotometer, a Qubit R3.0 Fluorometer, and an Agilent 2100 RNA Nano 6000 Assay Kit. Libraries were prepared according to the NEBNext R Ultra RNA Library Prep Kit for Illumina. To guarantee the data quality, the useful Perl script was used to filter the original data. The reference genomes and the annotation file were downloaded from the Ensembl database. Bowtie2 v2.2.3 was used to build the genome index, and clean data were then aligned to the reference genome using HISAT2 v2.1.0. The reads count for each gene in each sample was counted by HTSeq v0.6.0, and fragments per kilobase million mapped reads (FPKM) were then calculated to estimate the expression level of the genes in each sample. DEGseq was used for differential gene expression analysis between two samples with non-biological replicates. A p-value was assigned to each gene and adjusted by Benjamini and Hochberg's approach to control for the false discovery rate.

Ultra-low-input native ChIP-seq of H3K4me3

Blastocysts were harvested from rats fed with the diet containing 0, 0.4% and 1.0% methionine, respectively. Ultra-low-input native ChIP was conducted according to the previous study with minor revised. Blastocysts were re-suspended in nuclear isolation buffer and then added with MNase digestion buffer. Chromatin was pre-cleared with 5 µL of 1:1 protein A: protein G Dynabeads and IP with 1 mg of H3K4me3 antibody-bead complexes overnight at 4°C. IP complexes were washed with low salt buffer and protein-DNA complexes were eluted in ChIP elution buffer for 1.5 h at 68°C. IP material was purified by phenol chloroform, ethanol-precipitated and raw ChIP materials was resuspended in Tris-HCl pH 8.0.

ChIP material was used for library construction using NEBNext Ultra II DNA kit according to the instructions. Amplified indexed libraries were pooled, size selected on a 2% agarose gel and diluted to a final concentration of 10 mM. Cluster generation and paired-end sequencing (100 bp reads) were performed on the Illumina cluster station and Illumina HiSeq 2000.

Serum methionine metabolism measurement

Serum from pregnant rats was analyzed for SAM, and SAH using the enzyme-linked immunosorbent assay (ELISA) kits. All samples were analyzed in duplicate in a single assay. The sensitivities of the assays were 0.1 ng/mL and 0.1 µmol/mL for SAM and SAH respectively. Intra- and inter-assay coefficients of variation (CV) were <10 and 15%, respectively.

Cytokines detection

Cytokines in serum and cell supernatant were detected using Luminex 200 system according to manufacturer's protocol.

Placenta collection

A total of 108 pregnant rats were assigned randomly into three groups with methionine levels at 0, 0.4%, and 1.0%. Pregnant rats were fed the treatment diet from day 1 to day 18 of pregnancy. One-third of the rats ($n = 12$) in each group were euthanized on days 12, 14, and 18 of pregnancy respectively by an intraperitoneal injection of 2.0% sodium pentobarbital (30 mg/kg). All the placentae were excised, washed in 0.9% saline, weighed and frozen immediately in liquid nitrogen, and stored at –80°C for analyses.

Western blotting analysis

Tissues and cells were homogenized in RIPA lysis buffer containing protease inhibitor cocktails. After 30 min of incubation, the homogenates were centrifuged at 14,000 g for 15 min at 4°C, and the supernatant fluid was collected and stored at –80°C. Protein concentrations were determined using a BCA protein assay kit. Equal amounts of proteins were electrophoresed on SDS-polyacrylamide gels and transferred to a PVDF membrane. The membranes were incubated with the primary antibodies overnight at 4°C. After being washed with TBST, the membranes were incubated with a secondary antibody for 2 h at room temperature. Chemiluminescence was detected with western blot Luminance Reagent using an ImageQuant LAS 4000 mini system and quantified by ImageJ software. The β-actin level was used as an internal control.

Transfections

For cotransfection of siRNA and plasmid DNA, 6 µg of DNA and 300 pmol of siRNA (23 nM final concentration) were combined and transfected with Lipofectamine 3000. The cells were treated with methionine at 48 h after transfection and harvested for further analysis.

Plasmid construction and dual-luciferase reporter assays

A cDNA-derived Eomes sequence was cloned into the EcoRI and KpnI sites of a pCMV vector. The IL-5 promoters were amplified and cloned into the EcoRI and KpnI sites of a pCMV luciferase reporter vector.

For the luciferase assay, HTR cells at approximately 80% confluence on plates were transfected with plasmid DNA using Lipofectamine 3000 according to the manufacturer's instructions. The cells were cotransfected with pRL-TK, an internal control plasmid encoding Renilla luciferase, to normalize the firefly luciferase activity of the reporter plasmids. The cells were harvested 24 h after transfection, and luciferase activity was measured using a Dual-Luciferase Reporter Assay System on a ModulusTM microplate luminometer.

Chromatin immunoprecipitation

The binding of EOMES to the IL-5 promoters was assessed according to the instructions provided with the ChIP Assay Kit. Briefly, HTR cells were digested and crosslinked with formaldehyde at a final concentration of 1% for 10 min at 37°C. Then, 10× glycine was added to quench the unreacted formaldehyde. The cell pellets were washed twice with cold PBS and lysed in SDS lysis buffer containing 1 mM phenylmethanesulfonylfluoride. Crosslinked DNA was sheared by sonication into 200- to 1000-bp fragments, as evaluated by 1% agarose gel electrophoresis. A volume of 1.8 mL of ChIP dilution buffer was added to 0.2 mL chromatin fragments, and then 70 µL of Protein A + G Agarose/Salmon Sperm DNA was added and turned slowly overnight at 4°C. Then, 0.2 mL of the chromatin fragments was saved for later use as no precipitated total chromatin (input). The remaining chromatin fragments were incubated with 1 µg of anti-EOMES antibody. Normal rabbit IgG was used as a negative control for nonspecific immunoprecipitation. The chromatin-antibody complexes were incubated with Protein A + G Agarose/Salmon Sperm DNA for 1 h at 4°C. The antibody/DNA complexes on the agarose beads were collected by centrifugation, and the beads were washed in a series of cold buffers in the following order: low salt immune complex wash buffer, high salt immune complex wash buffer, LiCl immune complex wash buffer and TE buffer. The beads were suspended in elution buffer, and the precipitated protein/DNA complexes were eluted from the antibodies/beads. The crosslinking of protein/DNA complexes was reversed to free the DNA by the addition of 5 M NaCl and incubation of the mixture at 65°C for 4 h followed by incubation with 0.5 M EDTA, 1 M Tris-HCl and 20 mg/mL proteinase K at 45°C for 1 h. Finally, the DNA was purified with spin columns and used for real-time PCR.

QUANTIFICATION AND STATISTICAL ANALYSIS

Numerical data were analyzed and displayed using GraphPad Prism 10.0. Two-group comparisons were performed using Student's t-tests and comparisons among three groups were analyzed using ANOVA and post hoc Fisher's LSD tests when indicated. Quantitative data were presented as mean ± SEM. *p*-values <0.05 were considered statistically significant. The 2D response surfaces plotted at the median of the remaining two axes are visualized using thin-plate splines in Design-Expert (v10.0.7). Western blot band densities and immunofluorescence staining were quantified with ImageJ software. Flow cytometry data analysis was performed using Flow Jo (V10.8.1). Enrichment cluster, pathway cluster was performed using Metacape (<http://metascape.org/gp/index.html#/main>). The number of replicates for a given experiment was indicated in each figure legend.